Evidence of a retinotopic organization of early visual cortex but impaired extrastriate processing in sight recovery individuals

Suddha Sourav Biological Psychology and Neuropsychology, University of Hamburg, Hamburg, Germany

Davide Bottari Biological Psychology and Neuropsychology, University of Hamburg, Hamburg, Germany; IMT School for Advanced Studies Lucca, Lucca, Italy

Ramesh Kekunnaya Jasti V Ramanamma Children's Eye Care Center, Child Sight Institute, LV Prasad Eye Institute, Hyderabad, India

Brigitte Röder Biological Psychology and Neuropsychology, University of Hamburg, Hamburg, Germany

Numerous studies in visually deprived nonhuman animals have demonstrated sensitive periods for the functional development of the early visual cortex. However, in humans it is yet unknown which visual areas are shaped to which degree based on visual experience. The present study investigated the functional organization and processing capacities of early visual cortex in sight recovery individuals with either a history of congenital cataracts (CC) or late onset cataracts (developmental cataracts, DC). Visual event-related potentials (VERPs) were recorded to grating stimuli which were flashed in one of the four quadrants of the visual field. Participants had to detect rarely occurring grating orientations. The CC individuals showed the expected polarity reversal of the C1 wave between upper and lower visual field stimuli at the typical latency range. Since the C1 has been proposed to originate in the early retinotopic visual cortex, we concluded that one basic feature of the retinotopic organization, upper versus lower visual field organization, is spared in CC individuals. Group differences in the size and topography of the C1 effect, however, suggested a less precise functional tuning. The P1 wave, which has been associated with extrastriate visual cortex processing, was significantly attenuated in CC but not in DC individuals compared to typically sighted controls. The present study thus provides evidence for fundamental aspects of retinotopic processing in humans being independent of developmental vision. We suggest that visual impairments in sight recovery individuals may predominantly arise at higher cortical processing stages.

Introduction

Visual deprivation in sensitive phases can permanently alter the ability of the brain to acquire visual functions, and induces far-reaching changes going beyond the visual system even if the absence of vision is only temporary (Lee & Whitt, 2015). Transient, bilateral visual deprivation after birth has been shown to cause wide-ranging impairments in visual acuity (Ellemberg, Lewis, Maurer, Lui, & Brent, 1999), stereopsis (Tytla, Lewis, Maurer, & Brent, 1993), face and object processing (Le Grand, Mondloch, Maurer, & Brent, 2001; Putzar, Hötting, & Röder, 2010; Röder, Ley, Shenoy, Kekunnaya, & Bottari, 2013; Sinha & Held, 2012), and global motion perception (Bottari et al., 2018; Hadad, Maurer, & Lewis, 2012).

However, not all visual functions seem to depend on visual input after birth to the same degree. For example, color perception has been reported to develop normally without developmental experience of color (Brenner, Cornelissen, & Nuboer, 1990; McKyton,

Citation: Sourav, S., Bottari, D., Kekunnaya, R., & Röder, B. (2018). Evidence of a retinotopic organization of early visual cortex but impaired extrastriate processing in sight recovery individuals. *Journal of Vision*, *18*(3):22, 1–17, https://doi.org/10.1167/18.3.22.

https://doi.org/10.1167/18.3.22 Received October 23, 2017; published March 29, 2018 ISSN 1534-7362

Ben-Zion, Doron, & Zohary, 2015). Similarly, the neural systems of biological motion detection have been found to be indistinguishable in sight recovery individuals with a congenital onset of blindness and controls (Bottari et al., 2015; Hadad et al., 2012). Based on behavioral data in short and long deprived congenital cataract individuals, it has been proposed that congenital reversible blindness affects higher order visual processes more than basic visual functions (Le Grand et al., 2001; McKyton et al., 2015; Putzar, Hötting, Rösler, & Röder, 2007). In line with this proposal, event-related potentials (ERPs) in long-deprived sight recovery individuals were found to show a similar timing but indicated a lack of a functional specialization of face-selective processing of visual association areas (Röder et al., 2013).

Studies in nonhuman animals with a transient phase of congenital visual deprivation have described both structural anomalies including higher neural density, lower number of synapses per neuron, impaired cortico-tectal connectivity, lower size of the LGN, an atrophy of layers IV and V, and functional anomalies including a decreased responsiveness to visual stimulation and less well-defined receptive fields in the primary and secondary visual cortex (Berman, 1991; Sherman & Spear, 1982). In accord with recent human studies (e.g. Röder et al., 2013) the lack of response selectivity was particularly prominent in visual association areas such as the lateral suprasylvian cortex (Sherman & Spear, 1982). Nevertheless, some functional organization and selectivity has been found in visually deprived animals (see below) and it has been suggested that an initial functional organization emerges in the absence of vision but that the maintenance and future elaboration is dependent on visual input (Chapman, Gödecke, & Bonhoeffer, 1999).

The basic broad patterning of sensory area maps in the cerebral cortex is known to be strongly driven by transcription factor gradients (Grove & Fukuchi-Shimogori, 2003) and fine-tuned by spontaneous neural activity from the retina (Cang, Rentería, et al., 2005; Katz & Shatz, 1996). Even ocular dominance is partially installed by spontaneous activity from the retina (Katz & Crowley, 2002; Katz & Shatz, 1996). The majority of studies in visual deprivation have focused on early visual cortex, especially on areas 17 and 18. Hyvärinen, Carlson, and Hyvärinen (1981) found that despite some loss of visual responsiveness, Brodmann area 17 in Macaques remained highly responsive to visual stimuli even after a year of congenital, bilateral visual deprivation, whereas the number of visually activated neurons in extrastriate area 19 dwindled to less than 40% (Hyvärinen et al., 1981). Thus, the previous evidence suggests that while aberrant or absent environmental input to some degree might spare selected neural circuits at early cortical processing stages, visual functions higher up in the hierarchy may fail to develop properly due to an anomalous timing of environmental input or a lack of concerted development of neural structures (the *Sleeper effect*; Maurer, Mondloch, & Lewis, 2007, p. 45).

Numerous electrophysiological and brain imaging studies in humans have reported crossmodal recruitment of visual areas following blindness (Pavani & Röder, 2012; Renier, De Volder, & Rauschecker, 2014), which has been linked to crossmodal compensation in humans. Similarly, studies in nonhuman primates have found that even after a year following the end of visual deprivation, the trend of a higher representation of nonvisual processing in extrastriate areas further increased rather than decreased (Hyvärinen et al., 1981). Brain imaging studies in sight recovery humans have reported a stronger representation of auditory processing in the visual cortex (Collignon et al., 2015; Dormal et al., 2015; Guerreiro, Putzar, & Röder, 2015) in general decreasing with increasing duration of visual recovery (Dormal et al., 2015; Guerreiro, Putzar, & Röder, 2016b), suggesting that the crossmodal activation might partially but not fully retract following sight restoration.

Recent fMRI studies analyzing spontaneous BOLD (Blood-oxygen-level dependent) changes in congenitally permanently blind humans have repeatedly observed a retinotopically organized functional connectivity by and large indistinguishable from that of normally sighted humans (Bock et al., 2015; Striem-Amit et al., 2015). However, it is yet unknown whether the early visual cortex is capable of retinotopically organized *visual* processing in humans after sight restoration following congenital visual deprivation.

The present study used visual grating stimuli which were presented in the upper and lower visual fields. The locations of the stimuli were chosen to target the opposite banks of the calcarine sulcus, where the primary visual cortex is concentrated. The *C1 wave* is the first discernible wave in pattern-onset visual event-related potentials (VERPs), which has an onset of around 50 ms and peaks before 100 ms. The C1 wave shows a retinotopically determined polarity (Clark, Fan, & Hillyard, 1994; Jeffreys & Axford, 1972; Di Russo, Sereno, Pitzalis, & Hillyard, 2001): with average-referenced recording, visual stimuli in the upper visual field (UVF) elicit negative-going C1 waves, while visual stimuli originating in the lower visual field (LVF) elicit positive-going C1 waves. This polarity change is attributed to the functional mapping of the calcarine sulcus, where UVF and LVF are respectively mapped to the lower and the upper banks of the calcarine sulcus. We hypothesized to find evidence of a retionotopic organization in sight recovery individuals with a transient phase of congenital blindness; though based on the nonhuman animal literature, we predicted

Participant	Age	Sex	Cataract onset	Age at surgery	Visual acuity in the better eye (decimal)
CC-01	26 years	Male	Congenital	5 months	0.16
CC-02	37 years	Male	Congenital	24 months	0.50
CC-03	11 years	Male	Congenital	7 months	0.25
CC-04	13 years	Male	Congenital	4 months	0.33
CC-05	33 years	Male	Congenital	72 months	0.05
CC-06	23 years	Male	Congenital	4 months	0.10
CC-07	13 years	Male	Congenital	15 months	0.50
CC-08	8 years	Male	Congenital	1 month	0.63
CC-09	10 years	Male	Congenital	11 months	0.20
CC-10	18 years	Female	Congenital	25 months	0.33
DC-01	16 years	Male	Developmental	12 years	1.00
DC-02	19 years	Male	Developmental	14 years	1.00
DC-03	19 years	Male	Congenital nondense	17 years	0.13
DC-04	10 years	Male	Congenital nondense	6 years	0.08
DC-05	11 years	Female	Congenital nondense	3 years	0.40
DC-06	12 years	Female	Developmental	6 years	1.00
DC-07	11 years	Female	Developmental	8 years	0.40
DC-08	12 years	Male	Developmental	8 years	0.50

Table 1. Description of the congenital cataract (CC) and developmental cataract (DC) reversal individuals.

an overall lower visual responsiveness reflected in lower C1 amplitudes.

To access extrastriate processing, we assessed the second VERP wave, the positive-going P1, which has been localized to extrastriate areas 18/19 (Di Russo et al., 2001) and which does not show polarity reversals based on stimulus location. We hypothesized that extrastriate processing as indicated by the P1 wave is compromised in sight recovery individuals with a transient phase of congenital blindness evidenced by a lower P1 amplitude. We tested a group of participants who were born with total bilateral cataracts (referred to as CC) and subsequently underwent cataract-removal surgeries. In addition to the typically developed matched controls, another group of participants with incomplete congenital cataracts, or developmental cataracts (DC) was assessed. The DC group served to control for prevailing visual impairments and any effect related to a history of cataract. Participants saw circular visual gratings in four quadrants of the visual field while fixating in an oddball task, where rarely occurring grating orientations served as behavioral controls.

Method

Participants

Ten participants with a history of total dense bilateral congenital cataracts (CC; mean age: 19.2 years, range 8–37 years; one female, nine male; one left-handed) were tested at the LV Prasad Eye Institute, Hyderabad, India (see Table 1). The duration of visual deprivation ranged from 1–72 months with a mean of 16.8 months in this group. The CC participants had a geometric mean visual acuity of 0.24 (range: 0.05–0.625). In addition, 10 individuals with a history of developmental cataracts or congenital but incomplete cataracts (DC) took part in the study in the same institute. Incomplete data of two of the DC participants were discarded, resulting in one case because the participant wished to abort the experiment shortly after the beginning and in the other case because the participant could not fixate. The remaining eight participants (see Table 1) had a mean age of 13.8 years (range: 10–19 years; five male, three female; all right-handed) and a geometric mean visual acuity of 0.41 (range: 0.07–1.00). The mean age at surgery for DC individuals was 9.25 years (range: 3–17 years).

To compare visual acuities in the two cataract groups, the decimal values were converted to LogMAR units allowing a meaningful comparison of arithmetic means (Holladay, 1997). An independent-samples t test did not reveal a significant difference in visual acuity between the CC and the DC group: $t(16) = 1.275$, $p = 0.221$. CC and DC participants did not have any impairment in other sensory systems, or any known neurological disorder.

Matched control participants for the CC individuals (MCC) and DC individuals (MDC) were recruited at the University of Hamburg, Germany. The control participants were matched for age, sex, and handedness. Mean age of the MCC group ($N = 10$) was 18.3 years (range: 7–34 years), and mean age of the MDC

group was 14.3 years ($N = 8$, range: 10–21 years). Sex and handedness characteristics in the MCC and the MDC group were identical respectively to the CC and DC group. The control participants had normal or corrected-to-normal vision, no history of atypical development of the sensory systems, and did not report any neurological disorder.

The participants provided written informed consent for taking part in the study. For minor participants a legal guardian provided additional written informed consent. In case of the participants tested in the LV Prasad Eye Institute in Hyderabad, India, the information was conveyed in one of the languages the participant could understand. The study was approved by the Local Ethical Commission of the Faculty of Psychology and Movement Sciences, University of Hamburg, Germany, as well as the Institutional Ethical Review Board of LV Prasad Eye Institute, Hyderabad, India. The study conformed to the ethical principles outlined in the *Declaration of Helsinki*. Expenses associated with taking part in the study (e.g., travel costs) were reimbursed, and some monetary compensation was provided to adults. Minors received a small present.

Stimuli

The stimuli consisted of circular grating patterns subtending an angle of 2.5° which were flashed for 150 ms in one of the four visual field quadrants at an eccentricity of 4°. The visual stimuli were flashed one at a time. The grating patterns were black-and-white stripes with a spatial frequency of 2 cycles/°. Either horizontally oriented (80%), or vertically oriented (20%) gratings were displayed, whereby the rare vertically oriented trials served as behavioral targets. Interstimulus interval ranged from 1.5–2.2 s (mean: 1.85 s), chosen by a discrete uniform random variable with 10 ms steps. There were 128 trials in each of the four conditions.

The stimuli were presented at an angle of 25° in the upper visual field (UVF) quadrants, and at an angle of 45° in the lower visual field (LVF) quadrants (see Figure 1). These positions target symmetrically opposing banks of the calcarine sulcus since the horizontal meridian of the visual field is mapped not onto the base of the sulcus, but onto its lower bank (Aine et al., 1996; Di Russo et al., 2001).

Apparatus and procedure

The stimuli were presented on a 23-in. Samsung P2370 monitor at the University of Hamburg, and on a 20-in. Dell IN2030M monitor at LV Prasad Eye Institute. Both monitors had a refresh rate of 60 Hz and a typical luminance value of 250 cd/m^2. The experiment was programmed in Python using the PsychoPy framework version 1.83 (Peirce, 2008; http://www.psychopy.org).

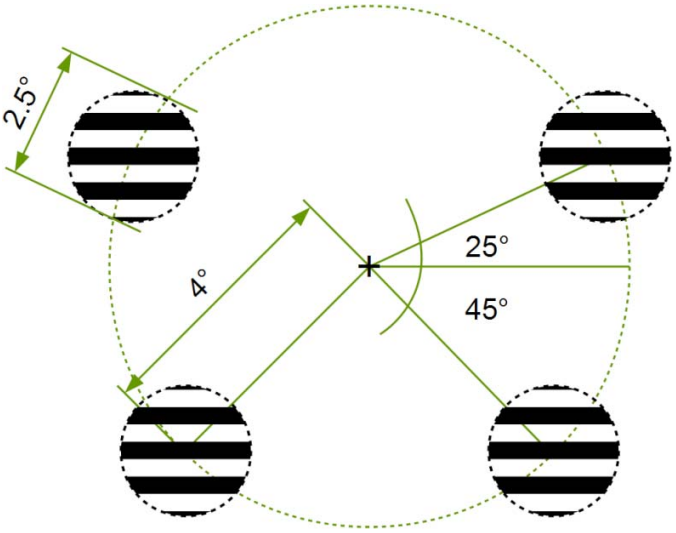

Figure 1. Locations of the four visual stimuli used in the experiment. The stimuli were presented one at a time with either vertical or horizontal stripes.

Participants sat at a distance of 45 cm from the monitor and were instructed to fixate on a central fixation cross. They were asked to respond in a nonspeeded manner to trials containing a vertically oriented grating pattern. A translator was present for participants who required the experiment to be explained in a language other than English or German. A demonstration block with a duration of five minutes, explaining all the steps, was run before collecting the data, and repeated if necessary until the participants understood the task.

Two of the 10 CC participants could not reliably differentiate between the horizontal and vertical grating orientations due to low visual acuity despite being able to perceive the flashes. We ensured that they could see the flashes by presenting single stimuli and asking for their location before starting recording of EEG data. These two participants passively viewed the stimuli.

Participants who were at least 15 years old used a foot pedal to respond by lifting their heel. Participants under 15 years of age responded verbally, and the response was entered by the experimenter via operating the foot pedal. The whole experiment, including preparing the electrode cap, took on average 2.5 hours. This overall duration was due to the experiment being comprised of additional parts which are not reported here.

EEG recording and preprocessing

EEG data were acquired with a custom 32-electrode EASYCAP elastic cap with sintered Ag/AgCl electrodes (EASYCAP GmbH, Herrsching, Germany), connected to a BrainAmp DC Amplifier (Brain Products GmbH, Gilching, Germany; http://www.brainproducts.com). Electrode arrangement was based on the standard 10–20 system and had the following recording locations: FP1, FP2, F7, F3, Fz, F4, F8, FC5, FC1, FCz, FC2, FC6, T7, C3, Cz, C4, T8, TP9, CP5, CP1, CP2, CP6, TP10, P7, P3, Pz, P4, P8, O1, O2, F9, and F10. EEG data were recorded referenced to the left earlobe at a sampling rate of 1 kHz through a hardware bandpass filter with a passband of 0.016–250 Hz.

Offline, the EEG data were preprocessed with EEGLAB toolbox version 11.5.4b (Delorme & Makeig, 2004) running on MATLAB version R2012b (MathWorks, Natick, MA). As a first step, power line noise at 50 Hz and its harmonics were filtered out with notch filters if interference from power line noise or switching power supplies was indicated by the presence of sharp peaks at these frequencies in the frequency domain. Typical biological artifacts due to blinks, eye movements, heartbeat, or extensive muscle activities were identified and eliminated using independent component analysis with the *runica* algorithm implemented in EEGLAB (Lee, Girolami, & Sejnowski, 1999; Onton & Makeig, 2006).

EEG data were average-referenced, lowpass-filtered with an upper cutoff frequency of 40 Hz and were epoched from −1,000 ms to 1,000 ms with respect to visual stimuli onsets. The epochs underwent a further automatic artifact rejection procedure based on the *pop_autorej* method implemented in EEGLAB that detects abnormal amplitude variations followed by a recursive rejection of epochs based on the distribution of amplitude values. Following this step, the electrodes for the left visual field stimuli were remapped, swapping the data for the left and right side electrodes. This is equivalent to mirroring the electrode locations with the midline electrodes as the axis of reflection. The VERPs to left visual field presentations were then averaged with the corresponding right visual field VERPs. In absence of a specific hypothesis about hemispheres, this provides effectively twice the number of trials, increasing the signal-to-noise ratio. As a result of the remapping of left visual field stimuli, we refer to the right side as the side ipsilateral to the stimuli, whereas the left side will be referred to as the contralateral side. Only epochs from standard trials, where participants did not respond to the stimuli, underwent ERP analysis.

Data analysis

Behavioral data

The hit rate and false positive rates of the CC and DC groups were compared with their control groups via separate independent-samples one-tailed *t* tests. We used one-tailed *t* tests based on the assumption that while the cataract participants' visual impairments could cause a performance reduction (i.e., lower hit rate and higher false positive rates), a performance increase would not be expected. The two CC individuals who saw the flashes, but could not reliably discriminate the grating orientations were not included in the analysis along with their controls. Thus, there were eight participants in each group (CC/MCC/DC/MDC) who entered the hit rate and false positive rate analyses.

In each of the four experimental groups (CC/MCC and DC/MDC), five participants responded verbally. The number of participants who responded with a foot pedal was three in the CC, DC, and MDC group, and five in the MCC group. We did not perform a reaction time (RT) analysis because of the low sample size (mean RT data of participants operating the foot pedal are reported in Supplementary Table S1).

ERP analysis

To investigate retinotopically determined polarity of the C1 wave, separate cluster-based permutation tests in each group (CC/MCC/DC/MDC) were run to compare VERPs elicited by LVF and UVF stimuli using the *FieldTrip* toolbox for MATLAB (Oostenveld, Fries, Maris, & Schoffelen, 2011). These cluster-based permutation tests were run over a 50 ms time window spanning from 50 ms to 100 ms poststimuli and over 13 posterior electrodes (CP1/2, CP5/6, TP9/10, P3/4, P7/8, Pz, and O1/2). The a priori selection of time range and electrodes were based on the well-established spatio-temporal properties of the C1 wave, which emerges within 100 ms after stimulus presentation over parieto-occipital electrodes (Di Russo et al., 2001). We used cluster-based permutation tests to avoid the problem of multiple comparisons across a large number of electrodes and time points (Maris & Oostenveld, 2007).

To assay possible differences in the temporal course of retinotopical processing, we calculated the C1 effect by subtracting the VERPs of the UVF from the VERPs of the LVF condition at electrode O1 and compared the peak latency and half-amplitude latency of the C1 effect between the CC/MCC and DC/MDC groups by means of independent-samples *t* tests. The electrode O1 (contralateral occipital electrode) was selected because it was the posterior electrode where most participants

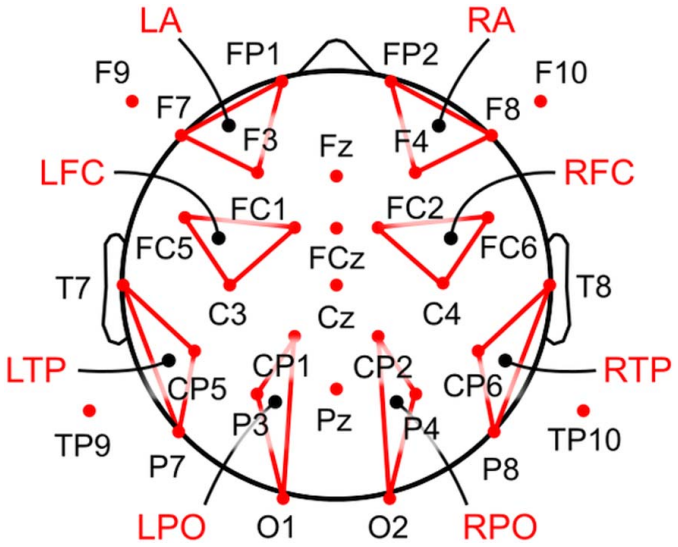

Figure 2. Schematic drawing of the electrode montage. Electrode clusters used in the analyses of normalized topographies are marked in red. Note that electrodes F9, F10, TP9, and TP10 are depicted outside of the circle representing the midline from nasion to inion over earholes.

showed the C1 effect (all participants except one control participant from the MDC group). The half-amplitude latency is defined as the time taken to reach 50% of the peak amplitude of a wave, and is known to be a conservative temporal measure which is more reliable than peak or onset latencies (Smulders, Kenemans, & Kok, 1996). The C1 wave, being the first VERP wave, is not preceded by any other VERP activity. For this reason, the half-peak latency is especially useful and was used as a measure of the temporal course of the C1 effect.

Moreover, to examine topographical differences of the C1 effect, we performed a topographical analysis comparing the C1 effect in CC/MCC and DC/MDC groups by means of separate cluster-based permutation tests in the time range of 50–100 ms over the whole electrode montage. To investigate spatial differences in the generators of the C1 effect by controlling for possible amplitude effects, we performed a further statistical analysis of the topography after normalizing the average VERP responses in the latency range of 50–100 ms to z scores (McCarthy & Wood, 1985; Murray, Brunet, & Michel, 2008). The normalized VERPs were then averaged in four electrode clusters: anterior (A), fronto-central (FC), temporo-parietal (TP), and parieto-occipital (PO) in each hemisphere (see Figure 2). Each cluster comprised of three electrodes. The average normalized VERPs at the clusters were then analyzed by means of a three-way ANOVA with the within-subject factors *Hemisphere* (left and right) and *Cluster* (A, FC, TP, and PO), and the between-subject factor *Group* (CC and MCC or DC and MDC). We only report significant interactions involving the factor *Group*.

For the P1 wave, we followed a statistical approach similar to the C1 effect, with the following exceptions. First, the latency of the P1 wave was calculated by finding the largest P1 response in each subject among the 13 posterior electrodes via an automated script. The results were further verified by visually inspecting the data. The average peak latency for P1 over all four groups (CC, DC, MCC, and MDC) and the two stimulus locations (UVF and LVF) was 143 ms ($SE = 2$ ms, range: 92–178 ms; for only UVF stimuli: $M = 147$ ms, $SE = 3$ ms, range: 112–175 ms; for only LVF stimuli: $M = 139$ ms, $SE = 4$ ms, range: 92–178 ms). Mean amplitudes for each participant were extracted spanning ±25 ms around the average latency (118–168 ms poststimulus).

Second, since the polarity of the P1 does not vary with UVF versus LVF presentation, we limited our analysis to UVF stimuli which elicited P1 amplitudes over a larger number of electrodes and because the P1 had a higher amplitude for UVF than for LVF stimuli (see Figure 4). This observation was verified by comparing the P1 to UVF and LVF stimuli separately in each control group (MCC and MDC) via separate cluster-based analyses in the P1 time range including posterior electrodes ($ps < 0.05$ for both groups). In order to maximize the power for detecting group differences, we restricted the statistical analysis to UVF stimuli.

Results

Behavioral data

Although the CC individuals' ($N = 8$) hit rate was high, $M = 0.911$, $SE = 0.040$, range: 0.689–1.00, it was significantly lower compared to the hit rate of the MCC individuals: $N = 8$, $M = 0.997$, $SE = 0.003$, range: 0.970–1.00; one-tailed independent-samples t test: $t(7) = 2.171$, $p = 0.033$, $d = 1.086$. The degrees of freedom were adjusted from 14 to 7 based on Levene's test, indicating that the groups had unequal variances ($F = 11{,}572$, $p = 0.004$). In contrast, the hit rates of the DC group, $M = 0.856$, $SE = 0.069$, range: 0.450–1.00, and the MDC group, $M = 0.930$, $SE = 0.030$, range: 0.795–1.00, did not significantly differ, $t(14) = 0.987$, $p = 0.171$.

The false positive rates were not found to be significantly different between the CC, $N = 8$, $M = 0.044$, $SE = 0.022$, range: 0.004–0.169, and the MCC group, $N = 8$, $M = 0.023$, $SE = 0.013$, range: 0.002–0.113; $t(14) = 0.840$; $p = 0.208$; or between the DC, $M = 0.023$, $SE = 0.012$, range: 0.003–0.090, and the MDC

group, $M = 0.019$, $SE = 0.012$, range: 0–0.097; $t(14) = 0.252$; $p = 0.403$.

For the two CC participants who could not reliably discriminate the grating orientations, we ensured that they could fixate and localize the stimuli by asking them to indicate the locations of the stimuli presented in random quadrants in a separate practice block at the beginning of the experiment. Both of these participants were able to correctly indicate the quadrants where the stimuli were presented at least eight out of ten times.

C1 wave

Cluster based permutation tests between the 50–100 ms time range over posterior electrodes found a significant C1 effect (difference between UVF and LVF stimulation) in all four groups: $p(\text{CC}) = 0.007$, $p(\text{MCC}) = 0.013$, $p(\text{DC}) = 0.042$, and $p(\text{MDC}) < 0.001$. The cluster-based permutation tests indicated that the C1 effect was most pronounced over the occipito-parietal electrodes in the MCC and the MDC groups (see Figure 3 for topography and Figure 4 for VERPs at electrode O1). In both cataract groups (CC and DC) the C1 effect was slightly contralateral. In the DC group, the C1 effect was more focal and smaller in amplitude compared to the MDC group, whereas the CC group displayed a broader, more contralateral scalp distribution involving centro-parietal and occipital electrode locations compared to their matched controls.

The mean peak latency of the C1 effect was 88 ms, $SE = 5$ ms; range: 65–112 ms, and the mean half-peak latency was 66 ms, $SE = 6$ ms; range: 24–86 ms, in the CC group ($N = 10$). These latencies did not significantly differ from their control group MCC ($N = 10$), where the mean peak latency was 85 ms, $SE = 4$ ms; range: 70–108 ms; $t(18) = 0.500$, $p = 0.623$, and the mean half peak latency was 73 ms, $SE = 3$ ms; range: 59–89 ms; $t(18) = 0.900$, $p = 0.380$. Likewise in the DC group ($N = 8$), neither the peak latency of the C1 effect, $M = 97$ ms; $SE = 4$ ms, range: 82–115 ms, nor the half peak latency (83 ms; $SE = 4$ ms, range: 61–97 ms) significantly differed from the MDC group [$N = 7$ (note that one MDC participant did not show the C1 effect at electrode O1), $M = 93$ ms, $SE = 7$ ms, range: 71–119 ms, $t(13) = 0.455$, $p = 0.657$; $M = 76$ ms, $SE = 5$ ms, range: 58–95 ms; $t(13) = 1.066$, $p = 0.306$, respectively for peak and half-peak latencies].

C1 topography analyses

Comparing the topography of the C1 effect between the CC and the MCC group by cluster-based permutation test over the whole electrode montage, we found that in the latency range of 50–100 ms the amplitude of the C1 effect was significantly higher in the CC group compared to their controls ($p = 0.044$). This effect was most pronounced over contralateral parietal and occipital electrodes. In contrast, in the DC and the MDC group, cluster-based permutation test over the whole electrode montage revealed the amplitude of the C1 effect to be significantly reduced in the DC group ($p = 0.024$), with the effect being most pronounced over central electrodes (see Figure 5).

We investigated whether the topography differences predominantly reflected an amplitude difference of the C1 effect, or a genuine topography difference by using normalized scores of the C1 effect (mean amplitude of the C1 effect in the latency range of 50–100 ms poststimulus). A three-way ANOVA with the within-subject factors *Hemisphere* (left and right) and *Cluster* (A, FC, TP, and PO), and the between-subject factor *Group* (CC and MCC) revealed a significant *Hemisphere X Cluster X Group* interaction, $F(3, 54) = 3.349$, $p = 0.040$, as well as a significant *Hemisphere X Group* interaction, $F(1, 18) = 6.724$, $p = 0.002$, indicating genuine group differences in scalp topography between CC and MCC individuals. By contrast, the normalized topographies of the DC and the MDC groups did not significantly differ.

Posthoc independent samples t test for each cluster between the CC and the MCC group with Benjamini-Hochberg procedure for controlling the familywise error rate revealed that the LTP cluster in the CC group showed a significantly higher C1 effect compared to the MCC group, $t(18) = 3.746$, $p = 0.001$. Thus, we found evidence for a difference in the scalp distributions between CC and MCC groups, that is, the CC group displayed a stronger contralateral and overall broader scalp distribution of the C1 effect. In contrast, DC and MDC groups differed in the size of the C1 effect (the DC group had a lower C1 effect) but not in scalp topography.

P1 wave

We ran separate cluster based permutation tests in all four groups (CC/DC/MCC/MDC) to examine the existence of a P1 wave by comparing whether the P1 amplitude elicited by UVF stimuli was significantly different from zero. The cluster based permutation tests between 118–168 ms time range over posterior electrodes detected the presence of a P1 wave in the DC, MCC, and MDC groups as evidenced by the existence of positive clusters over the posterior electrodes in this latency range, $p(\text{DC}) = 0.003$, $p(\text{MCC}) < 0.001$, and $p(\text{MDC}) < 0.001$. In contrast, no significant positivity in this time range was detected in the CC group over the posterior electrodes. Thus, the P1 wave was highly attenuated in the CC group[1] (see Figures 6 and 9).

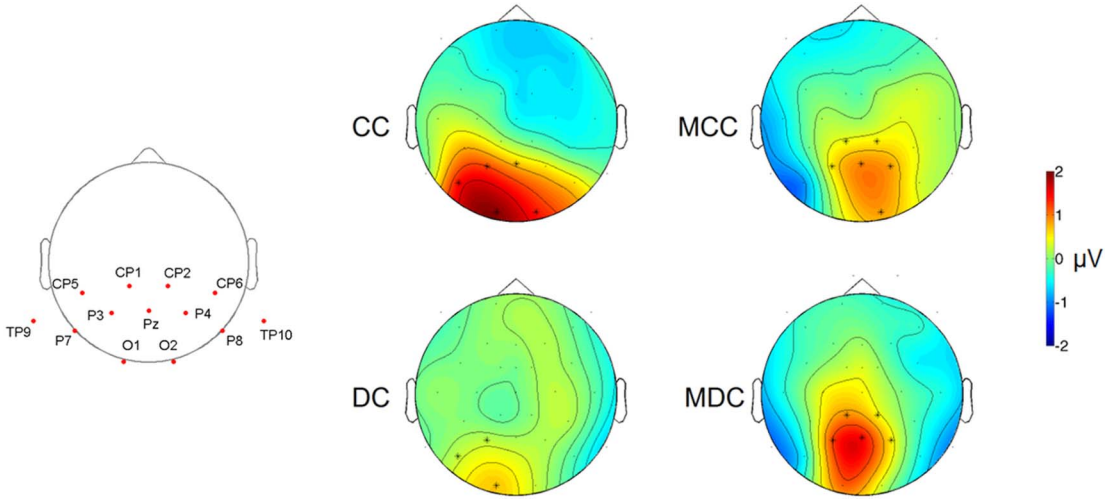

Figure 3. Topographic representation of the C1 effect. Left: A priori defined electrode locations selected for investigating the C1 effect. Note that electrodes TP9 and TP10 are depicted outside of the circle representing the midline from nasion to inion over earholes. Right: Topography of the C1 effect (difference between ERPs to LVF and UVF stimuli) between 50–100 ms poststimulus. In this latency range over posterior electrodes, cluster-based permutation tests revealed statistically significant C1 effects in all four groups (CC/DC/MCC/MDC, all *ps* $<$ 0.05). Asterisks indicate electrodes which survived tests for multiple comparison.

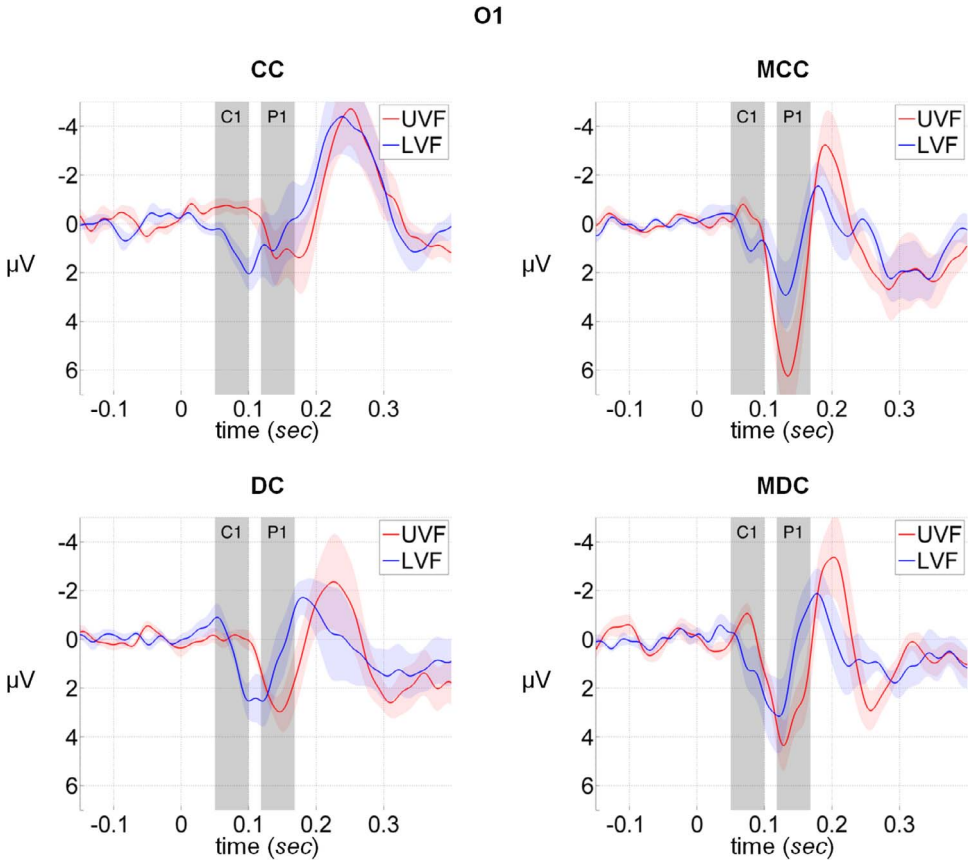

Figure 4. VERPs elicited at electrode O1. The four groups were congenital cataract group (CC), matched controls for the CC (MCC), developmental cataract group (DC), and matched controls for the developmental cataract group (MDC). C1 and P1 latency ranges are shaded. Error bands represent the standard error of the mean.

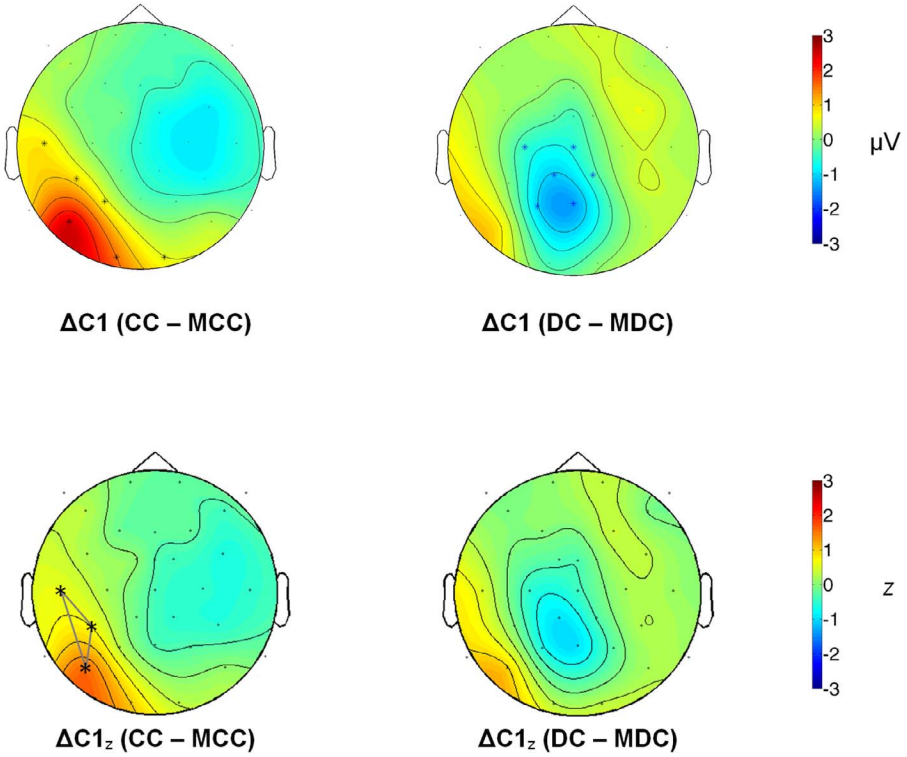

Figure 5. Topographic representations of the group differences in the C1 effect. Top Left: CC minus MCC difference of the C1 effect, averaged over the 50–100 ms poststimulus latency range (nonnormalized). Asterisks indicate the electrodes where the C1 effect significantly differed between groups. Top Right: DC minus MDC difference of the C1 effect, averaged over the 50–100 ms poststimulus latency range (nonnormalized). Bottom Left: Normalized topography of the difference of the C1 effect (CC–MCC) in the same latency range. Asterisks show the LTP cluster where the C1 effect was significantly higher in the CC group. Bottom Right: Normalized topography of the difference of the C1 effect (DC–MDC) in the same latency range.

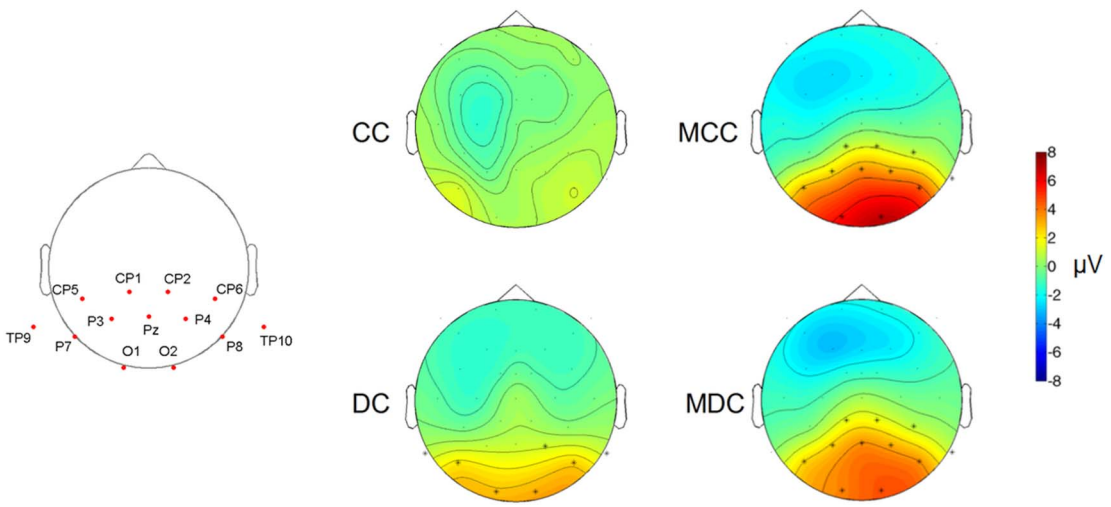

Figure 6. Topographic representation of the P1. Left: A priori defined electrode locations selected for investigating the existence of the P1 wave. Note that electrodes TP9 and TP10 are depicted outside of the circle representing the midline from nasion to inion over earholes. Right: Topography of P1 wave between 118–168 ms poststimulus. Asterisks indicate electrodes which survived tests for multiple comparisons.

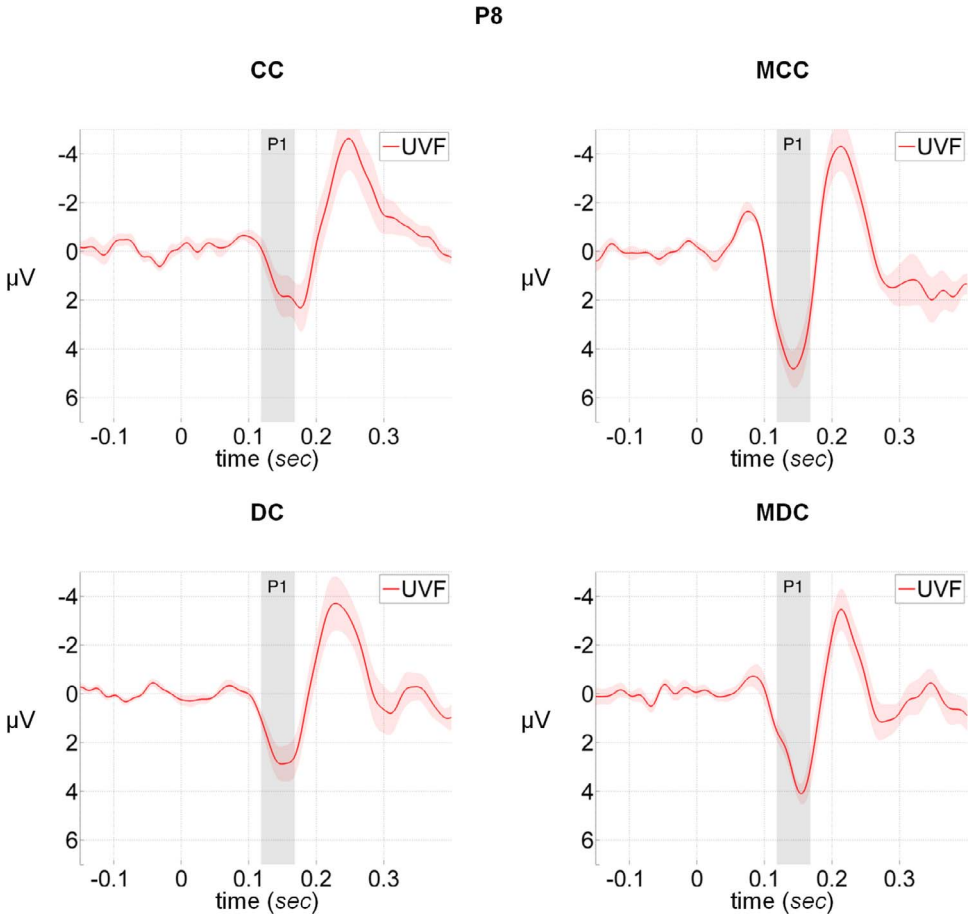

Figure 7. VERPs elicited by UVF stimuli at electrode P8. The four groups were congenital cataract group (CC), matched controls for the CC (MCC), developmental cataract group (DC), and matched controls for the developmental cataract group (MDC). P1 latency range is shaded. Error bands represent the standard error of the mean.

P1 topography analyses

Comparing the topography of the P1 wave between the CC and the MCC group by means of a cluster-based permutation test over the whole electrode montage in the latency range from 118–168 ms poststimulus found a significantly lower P1 amplitude in the CC group compared to the MCC group revealed by the existence of a posterior negative cluster ($p = 0.016$; see electrodes marked in red in Figure 8). A positive cluster corresponding to the negative part of the P1 wave topography in the MCC group compared to the CC group was found over frontal and fronto-central electrodes ($p = 0.015$).

In contrast, DC and MDC group did not differ over the posterior scalp ($p = 0.178$). However, a statistically significant higher positive group difference over the frontal and fronto-central electrodes ($p = 0.02$) was observed (see Figure 8).

To test for topographical differences, we first converted the average P1 amplitudes in the latency range from 118–168 ms poststimulus to normalized (z) scores over the whole electrode montage. Then, average z scores of eight electrodes clusters were calculated (see Figure 2) and submitted to a three-way ANOVA with the within-subject factors *Hemisphere* (left and right) and *Cluster* (A, FC, TP, and PO), and the between-subject factor *Group* (CC and MCC or DC and MDC).

In the CC and MCC groups, the ANOVA revealed a statistically significant *Cluster* × *Group* interaction, $F(3, 54) = 13.176$, $p < 0.001$. Posthoc independent samples t tests with Benjamini-Hochberg procedure to correct for false discovery rate revealed that at both left and right PO clusters, the MCC individuals had a significantly stronger P1 response than CC individuals, LPO: $t(18) = -3.875$, $p = 0.001$; RPO: $t(18) = -5.441$, $p < 0.001$. For the RA cluster a stronger negative response in MCC individuals was indicated ($t(18) = 3.605$, $p = 0.002$).

The ANOVA comparing the DC and the MDC groups revealed a significant *Cluster* × *Group* interaction, $F(3, 42) = 2.901$, $p = 0.046$. However, posthoc independent samples t tests with Benjamini-Hochberg procedure did not find any significant difference between groups at individual clusters.

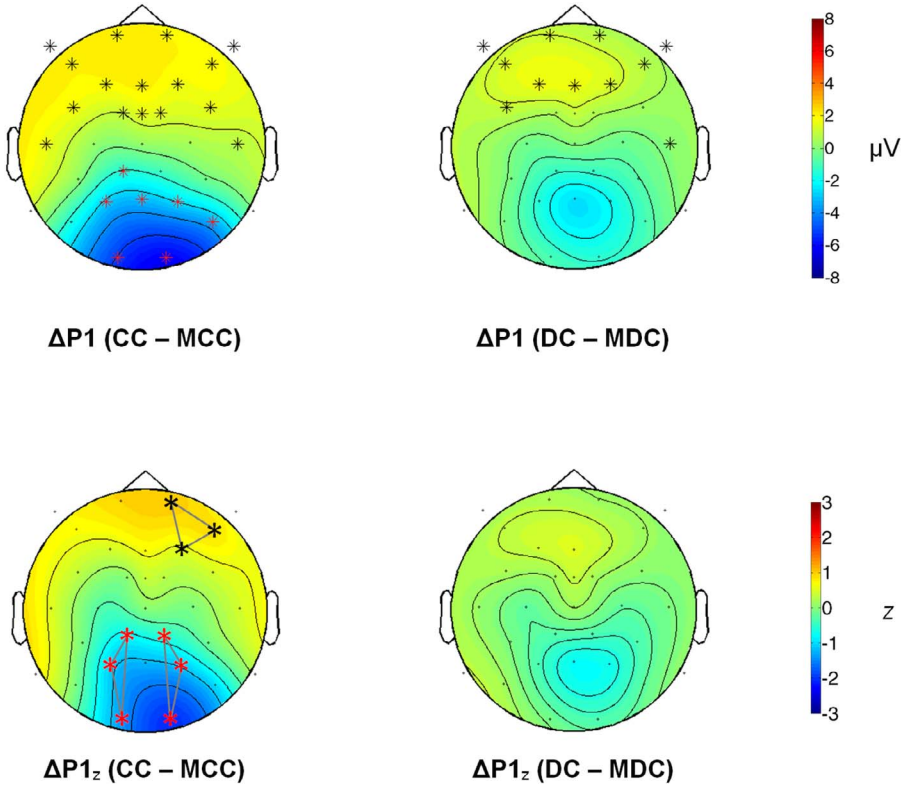

Figure 8. Topographic representations of the group differences of the P1. Top Left: CC minus MCC difference of the P1 wave, averaged over the 118–168 ms poststimulus latency range (nonnormalized). Asterisks indicate the electrodes where the topography significantly differed between groups. Top Right: DC minus MDC difference of the P1 wave, averaged over the 118–168 ms poststimulus latency range (nonnormalized). Asterisks indicate the electrodes where the topography significantly differed between groups. Bottom Left: Topography of the difference of the P1 (CC–MCC) in the same latency range after converting them to normalized (z) scores. Asterisks show the clusters where the topographies significantly differed. Bottom Right: Topography of the difference of the P1 (DC–MDC) in the same latency range after converting them to normalized (z) scores.

Discussion

The present study tested whether a basic feature of the retinotopic organization (upper vs. lower visual field organization) emerges in early visual cortex in sight recovery individuals with a history of congenital blindness, and to which degree the time-course of retinotopic processing recovers. Moreover, we assessed extrastriate processing to test the hypothesis that the experience dependence of cortical development increases from striate to extrastriate areas. Individuals with a history of congenital, dense bilateral cataracts (CC), individuals with developmental or congenital but not dense cataracts (DC), and typically developed matched controls (MCC as controls for the CC group, MDC as controls for the DC group) took part in the study. They were presented circular black-and-white grating stimuli appearing in one of the four quadrants of the visual field while electroencephalographic activity was recorded. We analyzed the C1 wave which has been proposed to originate in early, possibly primary visual cortex and which is sensitive to stimulus location (Jeffreys & Axford, 1972; Di Russo et al., 2001) along with the P1 wave, which has been shown to be generated by extrastriate areas. We found evidence that upper versus lower visual field representations in opposite banks of the calcarine sulcus, a hallmark of basic retinotopic organization, is spared after congenital visual deprivation. Moreover, processing in early visual cortex followed a typical time course. In contrast, extrastriate processing as indicated by the P1 did not seem to recover to the same degree following sight restoration.

Topological organizations seem to emerge quite early in development. A recent brain imaging study in nonhuman primates has found a basic retinotopic organization in the visual cortex at birth (Arcaro & Livingstone, 2017). In humans, using event-related potentials, Saby, Meltzoff, and Marshall (2015) demonstrated a somatotopic organization in somatosensory cortex in seven-month-old infants. The basic topographic organization of sensory cortices might even be independent of experience as a retinotopic organization in the occipital cortex has been observed in congenitally permanently blind humans (Striem-Amit et al., 2015)

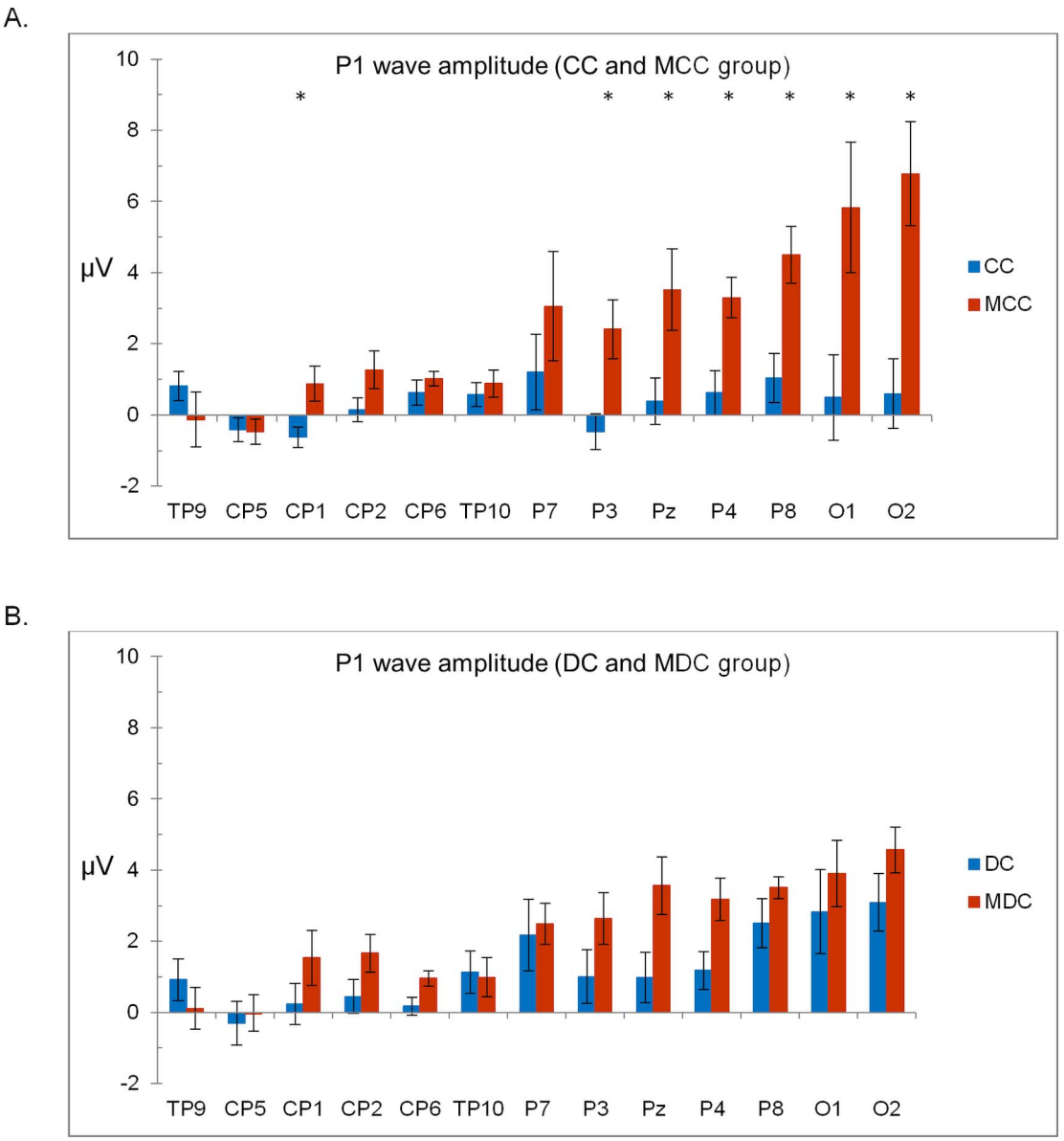

Figure 9. P1 amplitudes. (A) Mean P1 amplitudes (nonnormalized) in the latency range from 118–168 ms in the CC and the MCC group at the 13 electrodes posterior to the central line. Asterisks mark the electrodes from the cluster-based permutation test that survived multiple comparisons, showing that the P1 amplitude was larger in the MCC group compared to the CC group. (B) Mean P1 amplitude (nonnormalized) in the latency range from 118–168 ms in the DC and the MDC group.

and even in anophthalmic individuals (Bock et al., 2015). Nonhuman animal studies have indicated that the basic "blueprint" of patterning in the cerebral cortex seems to occur pre/perinatally in development (Grove & Fukuchi-Shimogori, 2003). In the visual system, such topographic mapping is known to be highly dependent on signaling molecules, with the *Eph-ephrin* receptors and ligands playing a key role in the formation of retinotopic maps (Cang, Kaneko, et al., 2005; Triplett & Feldheim, 2012). However, the maintenance and precise fine-tuning of the retinotopic maps over development probably depend on early visual experience. Our results are in accord with nonhuman animal studies demonstrating for the first time not only a retinotopic organization of human visual cortex after a transient phase of congenital blindness, but additionally that the early visual cortex is capable of processing *visual* stimuli with timing indistinguishable from that of typically developed sighted controls.

Recently Segalowitz, Sternin, Lewis, Dywan, and Maurer (2017) reported a reduced *N75* wave in CC individuals in a checkerboard pattern-reversal paradigm. The N75 in pattern-reversal VERP, like the C1 wave, is thought to originate in the striate cortex, suggesting a possible altered processing of visual

stimuli even at the early visual processing stage. However, the stimuli were not retinotopically presented and thus such changes suggested by a reduction of the N75 amplitude in the CC group are not indicative of a disrupted basic retinotopic processing. Indeed, Segalowitz et al. (2017) found the N75 amplitude in CC individuals to differ for different classes of simple texture stimuli, suggesting a not generally impaired early visual processing. Our results provide evidence that despite possible wide-spread changes in the visual cortex (Bavelier & Neville, 2002; Hyvärinen et al., 1981), key aspects of basic retinotopic organization and processing timing of visual stimuli can develop after congenital visual deprivation in humans.

At the same time, we found that the C1 effect in the CC group was larger in size and exhibited an altered topography compared to the MCC group. The increased C1 effect in the contralateral hemisphere compared to CC individuals was surprising since we expected a smaller C1 effect in the CC group due to nonhuman animal literature reporting degenerative processes in early visual cortex (Sherman & Spear, 1982). It has been suggested that sensory deprivation may cause an increase in excitatory mechanisms as a result of homeostatic changes in neuronal circuits, whereby the excitatory synapses increase their strength in absence of input (Turrigiano & Nelson, 2004). Moreover, an effect of congenital blindness on cortical structures is well known: Increased cortical thickness in occipital areas has been observed in both congenitally blind (Park et al., 2009; Qin, Liu, Jiang, & Yu, 2013) and CC individuals (Guerreiro, Erfort, Henssler, Putzar, & Röder, 2015). Guerreiro, Erfort, et al. (2015) argued that such changes might be driven by a lack of synaptic pruning, which is known to be experience-driven (Bourgeois, Goldman-Rakic, & Rakic, 2000).

Reduced synaptic pruning co-occurring with an incomplete establishment of inhibitory neural circuits might explain the topographical changes as indicated by the difference between the CC and the MCC groups in the normalized C1 effect. On the one hand, a lack of pruning might spread the visual stimulus driven activity to a larger number of neurons contralateral to the visual field in which the stimuli were presented. On the other hand, Bottari et al. (2016) reported that alpha oscillatory activity was significantly reduced in CC individuals compared to MC and DC individuals. Alpha activity has often been associated with the regulation of the excitatory/inhibitory balance of neural circuits and has been linked to inhibitory neural circuit activity (Jensen & Mazaheri, 2010). The elaboration of inhibitory neural circuits has been postulated as a hallmark of experience dependent functional tuning of neural systems (Hensch, 2004; Takesian & Hensch, 2013). Thus, it might be speculated that the elaboration of the mechanisms that allows for a fine tuning of neural activity was incomplete in the CC individuals, resulting in accord with nonhuman animal studies (Berman, 1991; Sherman & Spear, 1982) in a less precise functional tuning. As a consequence, despite the overall existence of a retinotopic organization in CC individuals which seems to be independent of visual experience (Bock et al., 2015; Striem-Amit et al., 2015), the retinotopic organization might be less precise in CC individuals.

In contrast, in the DC group, despite the C1 effect being smaller, no significant topographical change compared to the MDC group was observed, indicating that the observed effects in CC individuals were indeed due to a phase of transient blindness from birth. These results imply a sensitive phase for the precise tuning of neural circuits as previously demonstrated for higher order visual cortex (Röder et al., 2013).

The location of the visual stimuli and the subsequent analysis method employed in this study allow us to draw conclusions about the upper versus lower visual field organization but not with regard to other dimensions of retinotopy. For example, visual stimuli that are closer to the vertical meridian would be needed to study the left-right dimension of retinotopy, as symmetric C1 waves are expected to be elicited by visual stimuli crossing the vertical meridian (Clark et al., 1994).

We found a significantly lower P1 amplitude in the CC but not in the DC individuals compared to their controls, indicating that extrastriate processing might be strongly affected by a period of congenital visual deprivation. This finding is in accord with Bottari et al. (2015), who found a reduced P1 in CC individuals to moving dot stimuli. A reanalysis of a dataset by Röder et al. (2013) in the same article revealed a reduced P1 wave amplitude for the CC group compared to healthy controls for pictures of static face, house, and their scrambled versions as well. Thus, the reduction in the P1 wave amplitude in the CC group seems to hold across a wide range of stimulus classes, ranging from low-level stimuli as in the present study to object and dynamic stimuli. Since in the DC individuals we did not find a significant reduction of the P1 amplitude, we can exclude the possibility that the P1 reduction was predominantly driven by the effect of intraocular lenses or a general reduction of visual acuity as the CC and DC groups had similar visual acuities.

It is known that prestimulus phase alignment of alpha waves, and the phase relationship between the alpha and the theta waves play a significant role in generating the P1-N1 wave complex (Fellinger, Klimesch, Gruber, Freunberger, & Doppelmayr, 2011; Klimesch et al., 2004). The P1 wave has been hypothesized to be functionally closely related to alpha oscillations by Freunberger et al. (2008), who suggested that both alpha activity and the P1 wave might reflect

activity connected to the inhibition of neural systems related to "task-irrelevant brain areas or task-irrelevant stimulus categories" (p. 2339). As discussed above, Bottari et al. (2016, 2018) found evidence that alpha oscillatory activity is compromised in CC individuals, suggesting that the neural mechanisms regulating the excitatory-inhibitory balance might be compromised as a result of congenital visual deprivation. Such an imbalance might manifest itself not only as alpha oscillatory deficits, but additionally might underlie the generally reduced P1 amplitude. Transcranial direct-current stimulation, which has been posited to alter the excitatory-inhibitory balance in cortical circuits (Krause, Márquez-Ruiz, & Kadosh, 2013), has been reported to modulate P1 response (Accornero, Li Voti, La Riccia, & Gregori, 2007; Antal, Kincses, Nitsche, Bartfai, & Paulus, 2004). Thus, the P1 attenuation seen across stimulus classes, combined with the evidence of a compromised alpha activity in CC participants, might reflect a persistent excitatory-inhibitory imbalance as a result of congenital visual deprivation. Moreover, our work is consistent with the evidence of widespread changes in the extrastriate cortex following a period of visual deprivation (Hyvärinen et al., 1981), with the extrastriate cortex being less responsive to visual stimulation.

The P1 wave analyzed in the study, referred as *late P1* or *ipsi P1*, is thought to be originated in the fusiform gyrus anterior to area V4 (Di Russo et al., 2001). An integral part of the ventral stream, the fusiform gyrus is known to play a key role in differentiating and recognizing complex visual input such as faces (Kanwisher, McDermott, & Chun, 1997; Sergent, Ohta, & Macdonald, 1992) or words (Dehaene & Cohen, 2011). Thus, a reduced P1 might be associated with a general impairment in object processing (Maurer et al., 2007; see also Bottari et al., 2015; Röder et al., 2013).

Congenital visual deprivation is known to not only alter the typical development of the visual cortex, but to result in significant crossmodal changes in the (early) visual cortex as well. In congenitally blind individuals, activation of the (primary) visual cortex by the intact modalities and cognitive tasks has been observed (Kupers et al., 2011; Pavani & Röder, 2012; Renier et al., 2014). In CC individuals, evidence of auditory stimulus generated activity has been observed in retinotopic visual regions (Collignon et al., 2015; Guerreiro, Putzar, et al., 2015). However, such changes are unlikely to completely transfer crossmodal functions to the visual cortex (as suggested by Dormal et al., 2016) and might rather reflect a modulation of visual perceptions in a crossmodal context (Guerreiro, Putzar, & Röder, 2016a) In congenitally deaf cats, Land et al. (2016) found that despite considerable crossmodal reorganization, the neurons of the auditory cortex retained the ability to response to auditory stimuli after implantation of cochlear implants. Moreover, these authors found evidence for the visually driven neurons forming a separate subgroup from the auditory-driven neurons. Thus, crossmodal reorganization is unlikely to reassign the entire neural substrate of a modality to process information from intact modalities after sensory deprivation, especially at early processing stages like the C1 which is mainly driven by feedforward connections (Zhang & Luck, 2009) and whose neural substrates show considerable prenatal development (Cang, Kaneko, et al., 2005). Supporting this evidence, our study suggests that despite considerable reorganization of the (early) visual cortex and conspicuous changes in the later stages of visual processing, basic retinotopic processing is spared following congenital blindness. Our pattern of results are in agreement with a recent report in deaf cats: Whereas auditory-driven activity (via electric stimulation of the cochlea) at early latencies was indistinguishable in primary auditory cortex (A1) of congenitally deaf cats compared to hearing cats, significant group differences were observed for auditory association cortex (Yusuf, Hubka, Tillein, & Kral, 2017).

In conclusion, we found evidence for basic features of retinotopic processing in the early visual cortex being functional with a typical time-course after a period of bilateral congenital blindness, whereas extrastriate processing does not seem to recover to the same extent.

Keywords: visual development, event-related potentials, C1, retinotopy, visual cortex, congenital cataract, sight recovery

Acknowledgments

We are grateful to D. Balasubramanian for supporting the study at LV Prasad Eye Institute. We thank Rakesh Balachandar, Seema Banerjee, Larissa Brockmann, Giulia Dormal, Marlene Hense, and Lisa Stockleben for helping with data acquisition, and Maria Guerreiro for supporting participant recruitment. Rainer Schäfer and Dirk Waschatz provided technical assistance. The study was funded by the European Research Council grant ERC-2009-AdG 249425-*CriticalBrainChanges* and DFG Ro 2625/10-1 (BR).

Commercial relationships: none.
Corresponding author: Suddha Sourav.
Email: suddha.sourav@uni-hamburg.de.
Address: Biological Psychology and Neuropsychology, University of Hamburg, Hamburg, Germany.

Footnote

[1] Rerunning the same analysis for LVF stimuli revealed significant P1 waves for the MCC, DC, and MDC groups ($ps < 0.05$) but not for the CC group. The direct comparison between CC and MCC groups did, however, not reach significance level.

References

Accornero, N., Li Voti, P., La Riccia, M., & Gregori, B. (2007). Visual evoked potentials modulation during direct current cortical polarization. *Experimental Brain Research*, *178*(2), 261–266.

Aine, C. J., Supek, S., George, J. S., Ranken, D., Lewine, J., Sanders, J., … Wood, C. C. (1996). Retinotopic organization of human visual cortex: Departures from the classical model. *Cerebral Cortex*, *6*(3), 354–361.

Antal, A., Kincses, T. Z., Nitsche, M. A., Bartfai, O., & Paulus, W. (2004). Excitability changes induced in the human primary visual cortex by transcranial direct current stimulation: Direct electrophysiological evidence. *Investigative Opthalmology & Visual Science*, *45*(2), 702–707.

Arcaro, M. J., & Livingstone, M. S. (2017). A hierarchical, retinotopic proto-organization of the primate visual system at birth. *eLife*, *6*, e26196.

Bavelier, D., & Neville, H. J. (2002). Cross-modal plasticity: Where and how? *Nature Reviews. Neuroscience*, *3*(6), 443–452.

Berman, N. E. (1991). Alterations of visual cortical connections in cats following early removal of retinal input. *Brain Research. Developmental Brain Research*, *63*(1–2), 163–180.

Bock, A. S., Binda, P., Benson, N. C., Bridge, H., Watkins, K. E., & Fine, I. (2015). Resting-state retinotopic organization in the absence of retinal input and visual experience. *Journal of Neuroscience*, *35*(36), 12366–12382.

Bottari, D., Kekunnaya, R., Hense, M., Troje, N. F., Sourav, S., & Röder, B. (2018). Motion processing after sight restoration: No competition between visual recovery and auditory compensation. *NeuroImage*, *167*, 284–296.

Bottari, D., Troje, N. F., Ley, P., Hense, M., Kekunnaya, R., & Röder, B. (2015). The neural development of the biological motion processing system does not rely on early visual input. *Cortex*, *71*, 359–367.

Bottari, D., Troje, N. F., Ley, P., Hense, M., Kekunnaya, R., & Röder, B. (2016). Sight restoration after congenital blindness does not reinstate alpha oscillatory activity in humans. *Scientific Reports*, *6*, 24683.

Bourgeois, J.-P., Goldman-Rakic, P. S., & Rakic, P. (2000). Formation, elimination, and stabilization of synapses in the primate cerebral cortex. In M. S. Gazzaniga (Ed.), *The new cognitive neurosciences* (pp. 45–53). Cambridge, MA: MIT Press.

Brenner, E., Cornelissen, F., & Nuboer, W. (1990). Striking absence of long-lasting effects of early color deprivation on monkey vision. *Developmental Psychobiology*, *23*(5), 441–448.

Cang, J., Kaneko, M., Yamada, J., Woods, G., Stryker, M. P., & Feldheim, D. A. (2005). Ephrin-as guide the formation of functional maps in the visual cortex. *Neuron*, *48*(4), 577–589.

Cang, J., Rentería, R. C., Kaneko, M., Liu, X., Copenhagen, D. R., & Stryker, M. P. (2005). Development of precise maps in visual cortex requires patterned spontaneous activity in the retina. *Neuron*, *48*(5), 797–809.

Chapman, B., Gödecke, I., & Bonhoeffer, T. (1999). Development of orientation preference in the mammalian visual cortex. *Journal of Neurobiology*, *41*(1), 18–24.

Clark, V. P., Fan, S., & Hillyard, S. A. (1994). Identification of early visual evoked potential generators by retinotopic and topographic analyses. *Human Brain Mapping*, *2*(3), 170–187.

Collignon, O., Dormal, G., de Heering, A., Lepore, F., Lewis, T. L., & Maurer, D. (2015). Long-lasting crossmodal cortical reorganization triggered by brief postnatal visual deprivation. *Current Biology*, *25*(18), 2379–2383.

Dehaene, S., & Cohen, L. (2011). The unique role of the visual word form area in reading. *Trends in Cognitive Sciences*, *15*(6), 254–262.

Delorme, A., & Makeig, S. (2004). EEGLAB: An open source toolbox for analysis of single-trial EEG dynamics including independent component analysis. *Journal of Neuroscience Methods*, *134*(1), 9–21.

Di Russo, F., Sereno, M. I., Pitzalis, S., & Hillyard, S. A. (2001). Cortical sources of the early components of the visual evoked potential, *111*, 95–111.

Dormal, G., Lepore, F., Harissi-Dagher, M., Albouy, G., Bertone, A., Rossion, B., & Collignon, O. (2015). Tracking the evolution of crossmodal plasticity and visual functions before and after sight restoration. *Journal of Neurophysiology*, *113*(6), 1727–1742.

Ellemberg, D., Lewis, T. L., Maurer, D., Lui, C. H., &

Brent, H. P. (1999). Spatial and temporal vision in patients treated for bilateral congenital cataracts. *Vision Research*, *39*(20), 3480–3489.

Fellinger, R., Klimesch, W., Gruber, W., Freunberger, R., & Doppelmayr, M. (2011). Pre-stimulus alpha phase-alignment predicts P1-amplitude. *Brain Research Bulletin*, *85*(6), 417–423.

Freunberger, R., Höller, Y., Griesmayr, B., Gruber, W., Sauseng, P., & Klimesch, W. (2008). Functional similarities between the P1 component and alpha oscillations. *European Journal of Neuroscience*, *27*(9), 2330–2340.

Grove, E. A., & Fukuchi-Shimogori, T. (2003). Generating the cerebral cortical area map. *Annual Review of Neuroscience*, *26*(1), 355–380.

Guerreiro, M., Erfort, M. V., Henssler, J., Putzar, L., & Röder, B. (2015). Increased visual cortical thickness in sight-recovery individuals. *Human Brain Mapping*, *36*(12), 5265–5274.

Guerreiro, M., Putzar, L., & Röder, B. (2015). The effect of early visual deprivation on the neural bases of multisensory processing. *Brain*, *138*(6), 1499–1504.

Guerreiro, M., Putzar, L., & Röder, B. (2016a). Persisting cross-modal changes in sight-recovery individuals modulate visual perception. *Current Biology*, *26*(22), 3096–3100.

Guerreiro, M., Putzar, L., & Röder, B. (2016b). The effect of early visual deprivation on the neural bases of auditory processing. *The Journal of Neuroscience: The Official Journal of the Society for Neuroscience*, *36*(5), 1620–1630.

Hadad, B.-S., Maurer, D., & Lewis, T. L. (2012). Sparing of sensitivity to biological motion but not of global motion after early visual deprivation. *Developmental Science*, *15*(4), 474–481.

Hensch, T. K. (2004). Critical period regulation. *Annual Review of Neuroscience*, *27*(1), 549–579.

Holladay, J. T. (1997). Proper method for calculating average visual acuity. *Journal of Refractive Surgery*, *13*(4), 388–91.

Hyvärinen, J., Carlson, S., & Hyvärinen, L. (1981). Early visual deprivation alters modality of neuronal responses in area 19 of monkey cortex. *Neuroscience Letters*, *26*(3), 239–243.

Jeffreys, D. A., & Axford, J. G. (1972). Source locations of pattern-specific components of human visual evoked potentials. I. Component of striate cortical origin. *Experimental Brain Research*, *16*(1), 1–21.

Jensen, O., & Mazaheri, A. (2010). Shaping functional architecture by oscillatory alpha activity: Gating by inhibition. *Frontiers in Human Neuroscience*, *4*, e186.

Kanwisher, N., McDermott, J., & Chun, M. M. (1997). The fusiform face area: A module in human extrastriate cortex specialized for face perception. *The Journal of Neuroscience: The Official Journal of the Society for Neuroscience*, *17*(11), 4302–4311.

Katz, L. C., & Crowley, J. C. (2002). Development of cortical circuits: Lessons from ocular dominance columns. *Nature Reviews Neuroscience*, *3*(1), 34–42.

Katz, L. C., & Shatz, C. J. (1996, November 15). Synaptic activity and the construction of cortical circuits. *Science*, *274*(5290), 1133–1138.

Klimesch, W., Schack, B., Schabus, M., Doppelmayr, M., Gruber, W., & Sauseng, P. (2004). Phase-locked alpha and theta oscillations generate the P1–N1 complex and are related to memory performance. *Cognitive Brain Research*, *19*(3), 302–316.

Krause, B., Márquez-Ruiz, J., & Cohen Kadosh, R. (2013). The effect of transcranial direct current stimulation: A role for cortical excitation/inhibition balance? *Frontiers in Human Neuroscience*, *7*, e602.

Kupers, R., Beaulieu-Lefebvre, M., Schneider, F. C., Kassuba, T., Paulson, O. B., Siebner, H. R., & Ptito, M. (2011). Neural correlates of olfactory processing in congenital blindness. *Neuropsychologia*, *49*(7), 2037–2044.

Land, R., Baumhoff, P., Tillein, J., Lomber, S. G., Hubka, P., & Kral, A. (2016). Cross-modal plasticity in higher-order auditory cortex of congenitally deaf cats does not limit auditory responsiveness to cochlear implants. *Journal of Neuroscience*, *36*(23), 6175–6185.

Le Grand, R., Mondloch, C. J., Maurer, D., & Brent, H. P. (2001, April 19). Neuroperception: Early visual experience and face processing. *Nature*, *410*(6831), 890.

Lee, H.-K., & Whitt, J. L. (2015). Cross-modal synaptic plasticity in adult primary sensory cortices. *Current Opinion in Neurobiology*, *35*, 119–126.

Lee, T. W., Girolami, M., & Sejnowski, T. J. (1999). Independent component analysis using an extended infomax algorithm for mixed subgaussian and supergaussian sources. *Neural Computation*, *11*(2), 417–441.

Maris, E., & Oostenveld, R. (2007). Nonparametric statistical testing of EEG- and MEG-data. *Journal of Neuroscience Methods*, *164*(1), 177–190.

Maurer, D., Mondloch, C. J., & Lewis, T. L. (2007). Sleeper effects. *Developmental Science*, *10*(1), 40–47.

McCarthy, G., & Wood, C. C. (1985). Scalp distribu-

tions of event-related potentials: An ambiguity associated with analysis of variance models. *Electroencephalography and Clinical Neurophysiology*, *62*(3), 203–208.

McKyton, A., Ben-Zion, I., Doron, R., & Zohary, E. (2015). The limits of shape recognition following late emergence from blindness. *Current Biology*, *25*(18), 2373–2378.

Murray, M. M., Brunet, D., & Michel, C. M. (2008). Topographic ERP analyses: A step-by-step tutorial review. *Brain Topography*, *20*(4), 249–264.

Onton, J., & Makeig, S. (2006). Information-based modeling of event-related brain dynamics. *Progress in Brain Research*, *159*, 99–120.

Oostenveld, R., Fries, P., Maris, E., & Schoffelen, J.-M. (2011). FieldTrip: Open source software for advanced analysis of MEG, EEG, and invasive electrophysiological data. *Computational Intelligence and Neuroscience*, *2011*, 156869.

Park, H.-J., Lee, J. D., Kim, E. Y., Park, B., Oh, M.-K., Lee, S., & Kim, J.-J. (2009). Morphological alterations in the congenital blind based on the analysis of cortical thickness and surface area. *NeuroImage*, *47*(1), 98–106.

Pavani, F., & Röder, B. (2012). Crossmodal plasticity as a consequence of sensory loss: Insights from blindness and deafness. In B. E. Stein (Ed.), *The new handbook of multisensory processes* (pp. 737–759). Cambridge, MA: MIT Press.

Peirce, J. W. (2008). Generating stimuli for neuroscience using PsychoPy. *Frontiers in Neuroinformatics*, *2*, e10.

Putzar, L., Hötting, K., & Röder, B. (2010). Early visual deprivation affects the development of face recognition and of audio-visual speech perception. *Restorative Neurology and Neuroscience*, *28*(2), 251–257.

Putzar, L., Hötting, K., Rösler, F., & Röder, B. (2007). The development of visual feature binding processes after visual deprivation in early infancy. *Vision Research*, *47*(20), 2616–2626.

Qin, W., Liu, Y., Jiang, T., & Yu, C. (2013). The development of visual areas depends differently on visual experience. *PLoS One*, *8*(1), e53784.

Renier, L., De Volder, A. G., & Rauschecker, J. P. (2014). Cortical plasticity and preserved function in early blindness. *Neuroscience & Biobehavioral Reviews*, *41*, 53–63.

Röder, B., Ley, P., Shenoy, B. H., Kekunnaya, R., & Bottari, D. (2013). Sensitive periods for the functional specialization of the neural system for human face processing. *Proceedings of the National Academy of Sciences, USA*, *110*(42), 16760–16765.

Saby, J. N., Meltzoff, A. N., & Marshall, P. J. (2015). Neural body maps in human infants: Somatotopic responses to tactile stimulation in 7-month-olds. *NeuroImage*, *118*, 74–78.

Segalowitz, S. J., Sternin, A., Lewis, T. L., Dywan, J., & Maurer, D. (2017). Electrophysiological evidence of altered visual processing in adults who experienced visual deprivation during infancy. *Developmental Psychobiology*, *59*(3), 375–389.

Sergent, J., Ohta, S., & Macdonald, B. (1992). Functional neuroanatomy of face and object processing. *Brain*, *115*(1), 15–36.

Sherman, S. M., & Spear, P. D. (1982). Organization of visual pathways in normal and visually deprived cats. *Physiological Reviews*, *62*(2), 738–855.

Sinha, P., & Held, R. (2012). Sight restoration. *F1000 Medicine Reports*, *4*, e17.

Smulders, F. T. Y., Kenemans, J. L., & Kok, A. (1996). Effects of task variables on measures of the mean onset latency of LRP depend on the scoring method. *Psychophysiology*, *33*(2), 194–205.

Striem-Amit, E., Ovadia-Caro, S., Caramazza, A., Margulies, D. S., Villringer, A., & Amedi, A. (2015). Functional connectivity of visual cortex in the blind follows retinotopic organization principles. *Brain*, *138*(6), 1679–1695.

Takesian, A. E., & Hensch, T. K. (2013). Balancing plasticity/stability across brain development. *Progress in Brain Research*, *207*, 3–34.

Triplett, J. W., & Feldheim, D. A. (2012). Eph and ephrin signaling in the formation of topographic maps. *Seminars in Cell & Developmental Biology*, *23*(1), 7–15.

Turrigiano, G. G., & Nelson, S. B. (2004). Homeostatic plasticity in the developing nervous system. *Nature Reviews Neuroscience*, *5*(2), 97–107.

Tytla, M. E., Lewis, T. L., Maurer, D., & Brent, H. P. (1993). Stereopsis after congenital cataract. *Investigative Ophthalmology & Visual Science*, *34*(5), 1767–1773.

Yusuf, P. A., Hubka, P., Tillein, J., & Kral, A. (2017). Induced cortical responses require developmental sensory experience. *Brain*, *140*(12), 3153–3165.

Zhang, W., & Luck, S. J. (2009). Feature-based attention modulates feedforward visual processing. *Nature Neuroscience*, *12*(1), 24–25.